Spin correlations in the triangular-lattice random mixed antiferromagnet

1998 J. Phys.: Condens. Matter 10 4057

(http://iopscience.iop.org/0953-8984/10/18/015)

J. Phys.: Condens. Matter **10** (1998) 4057–4070. Printed in the UK PII: S0953-8984(98)90601-4

Spin correlations in the triangular-lattice random mixed antiferromagnet

Y Todate†, C Kikuta†, E Himoto†, M Tanaka† and J Suzuki‡

† Department of Physics, Faculty of Science, Ochanomizu University, Otsuka, Bunkyo-ku, Tokyo 112, Japan

‡ Neutron Scattering Laboratory, JAERI, Tokai, Ibaraki 319-11 Japan

Received 12 January 1998

Abstract. Spin-glass-like freezing in the triangular-lattice random mixed antiferromagnet $YFeMnO_4$ has been analysed by Monte Carlo simulation. Experimental results on random diluted $LuGaMnO_4$ have also been presented. The analysis provides a qualitative interpretation of the experimentally observed spin freezing in the random mixed system $YFeMnO_4$ as well as the diluted systems $LuGaMnO_4$ and $LuFeMgO_4$. The non-uniform antiferromagnetic interaction due to the random distribution of Mn^{2+} and Fe^{3+} in $YFeMnO_4$ prevents long-range spin ordering, but instead it causes well-defined short-range correlation and a distribution of the relaxation time. The simulation demonstrates the formation of a higher-order structure of the short-range correlation at low temperatures. The development of a long-range correlation of quasi-static spins at the cusp temperature of the susceptibility is discussed.

1. Introduction

It is now widely recognized that a spin-freezing phenomenon similar to that exhibited by spin glasses occurs when random magnetic defects or impurities are introduced in antiferromagnetic compounds which are based on structures such as triangular- [1, 2], kagomé- [3] or tetrahedral-network lattices [4, 5]. Theoretical studies have also suggested that randomly diluted antiferromagnets with geometrical frustration inherent in the lattice show spin-glass-like freezing [6, 7]. Recently, with this in mind, we presented a report [8] (hereafter denoted as I) in which the randomly diluted triangular-lattice antiferromagnet $LuFeMgO_4$, which shows clear spin-glass-like behaviour, is investigated. Comparing a Monte Carlo simulation with experimental results on $LuFeMgO_4$, we have presented a microscopic description of the freezing. Although it has been argued that there is no finite-temperature transition in any short-range spin glasses in two dimensions [9–11], our analysis of cooperative freezing in a quasi-two-dimensional random frustrated system based on a two-dimensional model seems to be sufficient for interpreting the experimentally observed freezing at 33 K in $LuFeMgO_4$. In the experimental sense, we consider the observed (or simulated) cusp temperature of the susceptibility as the point at which some long-range spin correlation is detected, at least on the timescale of our observation. It would be valuable to evolve a study of this cooperative freezing in this random frustrated system, since, in our view, essentially the same physics as for conventional spin glasses applies.

In this report we present an analysis of another prototype random frustrated system, $YFeMnO_4$, which also shows clear spin-glass-like behaviour and in which the frustrating 'non-uniform' antiferromagnetic interactions on the triangular lattice seem to cause this

0953-8984/98/184057+14$19.50

glass-like behaviour. A random diluted system, $LuGaMnO_4$, has also been studied with the aim of obtaining consistent models for three random frustrated systems: the diluted Fe^{3+} system, the diluted Mn^{2+} system, and the Fe^{3+}–Mn^{2+} mixed system.

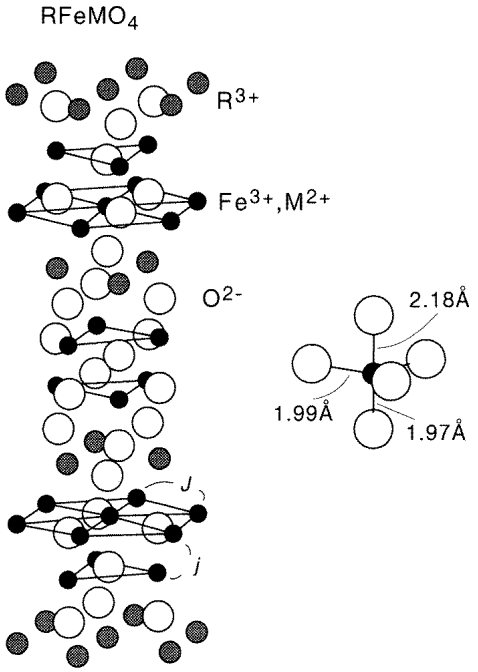

Figure 1. The crystal structure of RFe_2O_4-type oxides. The local structure in which the transition metal ion is surrounded by five oxygen ions is also shown. The distances between the metal ion and the oxygen ions are the values determined for YFe_2O_4.

The oxides studied here are insulators, and have RFe_2O_4-type layered hexagonal (rhombohedral) structure [12, 13] in which adjacent pairs of triangular nets of magnetic ions form an undulating honeycomb lattice (figure 1). $YFeMnO_4$ is a mixed antiferromagnet in which two different magnetic ions, Fe^{3+} and Mn^{2+}, are randomly distributed on the triangular lattice in the ratio 1:1. Spins in these compounds can be treated as Heisenberg ones with $S = \frac{5}{2}$. The magnetic properties reported so far for $LuFeMgO_4$ and $YFeMnO_4$ are characterized by anisotropic spin-glass-like behaviour [14, 15]. The dc susceptibilities of these two compounds show clear spin-glass-like cusps at 33 and 60 K, respectively, and typical cooling-field dependences appear below the temperatures at which these cusps occur, T_{cusp}. The ac susceptibilities also show spin-glass-like behaviour [1]. $\chi(T)$ is anisotropic for these compounds: $\chi_{\parallel}$ with $\boldsymbol{H}_{\mathrm{ext}}$ parallel to the $c(z)$-axis is always larger than $\chi_{\perp}$ for $T \lesssim 5T_{\mathrm{cusp}}$.

A short-range spin correlation based on the triangular 120° structure is commonly seen in these compounds [8, 16, 17]. Although the short-range correlation observed in neutron scattering experiments does not show any anomaly at the cusp temperature, it plays an important role in this study. In order to interpret these experimental findings, as in I, we perform a Monte Carlo simulation of the random mixed system and discuss the spin freezing in $YFeMnO_4$.

First, experiments on $LuGaMnO_4$ will be presented, because information about the

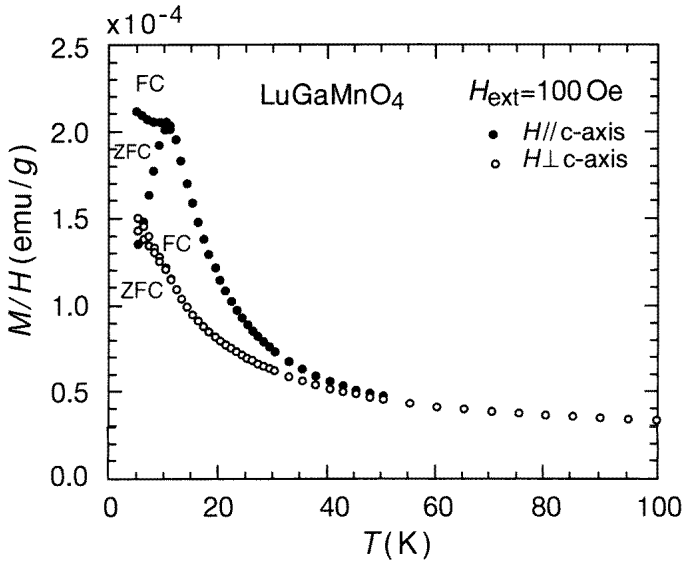

Figure 2. The temperature dependence of the dc susceptibility of $LuGaMnO_4$. A cusp occurs at 11 K in the zero-field-cooled $\chi_{\|}(T)$.

exchange interaction J_{MnMn} between Mn^{2+} ions is required in addition to information on J_{FeFe}. Then, using the values of J_{FeFe} and J_{MnMn} determined, the random mixed system $YFeMnO_4$ (or $LuFeMnO_4$) will be analysed.

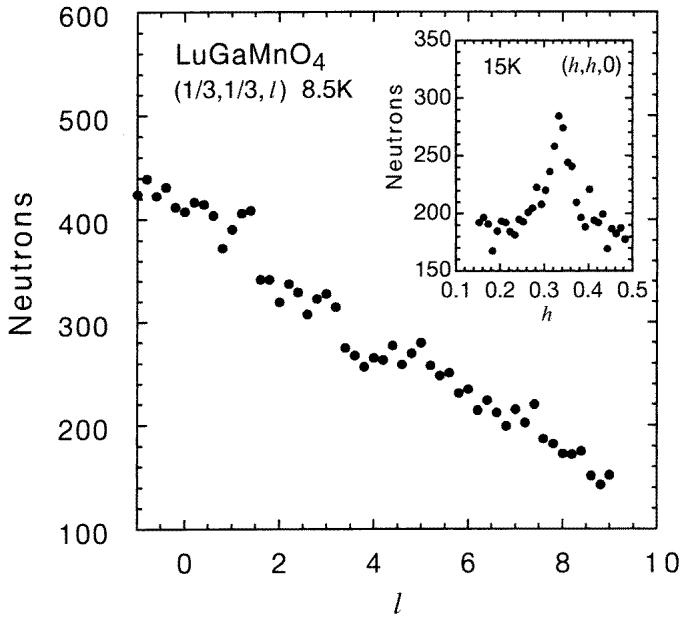

Figure 3. The neutron elastic scattering intensity measured along $(\frac{1}{3}, \frac{1}{3}, \ell)$ and $(h, h, 0)$ (inset).

2. Experimental results; $LuGaMnO_4$

$LuGaMnO_4$ was synthesized from a mixture of starting materials: 99.9% pure Lu_2O_3, 99.9% pure MnO and 99.99% pure Ga_2O_3 at 1400 °C under a controlled atmosphere of a CO_2–H_2 mixture gas. Single crystals were grown by the conventional floating-zone method from a sintered rod of powdered $LuGaMnO_4$. Figure 2 shows the DC susceptibility of the single crystal measured by a SQUID magnetometer under an external field of 100 Oe. A clear cusp is shown at $T_{\rm cusp} = 11$ K in $\chi_{\parallel}(T)$, and below $T_{\rm cusp}$ a cooling-field dependence is observed. There is no detectable cusp in $\chi_{\perp}(T)$, and the difference between the field-cooled and zero-field-cooled values is small. This feature is also shown by $LuFeMgO_4$ [1, 14], but with a higher freezing temperature ($T_{\rm cusp} = 33$ K for $LuFeMgO_4$).

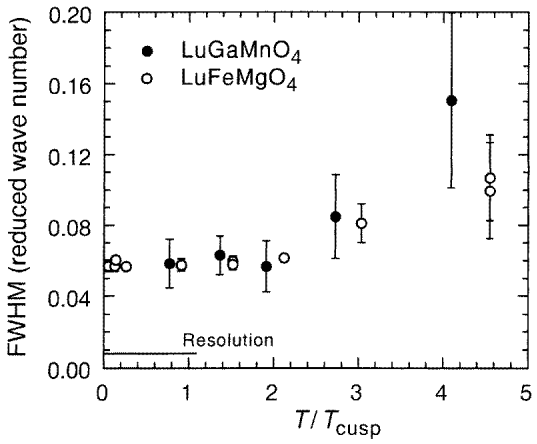

Figure 4. The temperature dependence of the widths of the $(\frac{1}{3}, \frac{1}{3}, 0)$ diffuse peak for $LuGaMnO_4$ and $LuFeMgO_4$. The temperature is normalized with respect to $T_{\rm cusp}$.

Neutron scattering measurements were carried out on the TAS-2 spectrometer at JRR-3M (JAERI, Tokai, Japan). Since a large single crystal was not available, several pieces of small ($\approx$25 mm^3) single crystals were mounted on a holder. Figure 3 shows the elastic scattering intensity measured along $(\frac{1}{3}, \frac{1}{3}, \ell)$ and $(h, h, 0)$. Short-range spin correlation characterized by the diffuse $(\frac{1}{3}, \frac{1}{3}, \ell)$ ridge has been observed at temperatures below 45 K, which is considerably higher than $T_{\rm cusp}$. The scan along ℓ shows that the correlation between the layers which compose the bilayer is weak. The temperature dependence of the width of the diffuse $(\frac{1}{3}, \frac{1}{3}, 0)$ peak in $LuGaMnO_4$ is compared with the corresponding results for $LuFeMgO_4$ [8] in figure 4. Note the identical correlation lengths ($\xi \simeq 9.5$ Å) for the two compounds at low temperatures. The short-range correlation length appears to be dependent only on the geometrical connectedness of the magnetic ions in this diluted system, with the magnetic ion concentration $c = 0.5$. This experiment shows that the behaviour of the spins in $LuGaMnO_4$ is essentially the same as in the case for $LuFeMgO_4$.

3. Monte Carlo simulation

The Monte Carlo simulation, assuming classical Heisenberg spins with one-ion axial anisotropy, has provided a qualitative explanation of the magnetic properties of the diluted

system $LuFeMgO_4$. The assumed model Hamiltonian is

$$\mathcal{H} = \sum_{\langle i,j \rangle} J_{ij} \boldsymbol{S}_i \cdot \boldsymbol{S}_j - D \sum_i (S_i^z)^2 + j \sum_{\langle i,k \rangle} \boldsymbol{S}_i \cdot \boldsymbol{S}_k \tag{1}$$

where J and j are the magnitudes of the nearest-neighbour antiferromagnetic interactions within the triangular layer and between the layers, respectively, and D is the anisotropy constant.

For the analysis of $YFeMnO_4$, however, the model needs slight modification, because a preliminary analysis using (1) was not sufficient in view of the following two features:

(i) the $z(c)$- and xy- (in-plane) components of the spins form a cusp at the same temperature in $YFeMnO_4$, while the Hamiltonian (1) gives different freezing temperatures for the z- and xy-components; and

(ii) Mössbauer measurements [14] suggest that the spin direction of Fe^{3+} is nearly isotropic in $YFeMnO_4$ at the lowest temperature, but the simulation using (1) shows a substantial difference between the z- and xy-components.

The discrepancy is partly removed if an in-plane anisotropy is included in addition to the axial one, D. It is fairly reasonable to include the in-plane anisotropy, since the strong frustration forces spins to form non-collinear local structure, and the anisotropy within the c-plane is responsible for the degree of freedom of the xy-components. Considering the fact that each of the magnetic ions is surrounded by three oxygen ions in the c-plane as shown in figure 1, we assume the in-plane anisotropy energy term to be

$$\mp \frac{1}{2} G((S_x + \mathrm{i}S_y)^3 + (S_x - \mathrm{i}S_y)^3) = \mp G(S_x^3 - 3S_x S_y^2) \tag{2}$$

where the minus and plus signs correspond to the spins on the upper and lower layers, respectively. Note that the time-reversal symmetry of the Hamiltonian is maintained because the axis is reversed in the lower layer. As regards the rather strong anisotropy found for Mn^{2+} and Fe^{3+}, it is worth noting that the strong anisotropy for Fe^{3+} is also found in a hexagonal magnetoplumbite [18] and that the situation is nearly the same as in the present case in which the crystal structure leads to low-symmetry coordination of the anions.

Further modification of the model Hamiltonian may be possible by taking into account the dipolar interaction and/or higher-order anisotropic exchange interactions which specify the coupling between different spin components, in order to reproduce the simultaneous freezing of the z- and xy-components in $YFeMnO_4$. We have not included such anisotropic interactions in this study, however, mainly because of the increase in the computation time required that would ensue and because of the difficulty of discussing detailed exchange interactions in the strongly disordered local environment in the oxides. Except the simultaneous freezing of the z- and xy-components—as will be shown later in this section—the experimentally observed magnetic properties of $YFeMnO_4$ are reproduced by this simulation. Since there is no qualitative difference between the z- and xy-components as regards the simulated freezing properties, we discuss the freezing in this random mixed system on the basis of the Hamiltonian (1) and (2). At the present stage, the model seems to be sufficient for qualitative interpretation of the spin freezing in this random mixed system. It should also be mentioned that the introduction of the in-plane anisotropy does not lead to any qualitative change in the simulated results for the diluted system.

For the analysis of $YFeMnO_4$, a set of parameters have been roughly estimated by comparing the freezing temperature and the anisotropy for the three compounds $LuFeMgO_4$, $LuGaMnO_4$, and $YFeMnO_4$. As noted in the introduction, we consider T_{cusp} as the temperature at which some change in the spin correlation is detected on the timescale of our

Table 1. The experimentally observed $T_{\rm cusp}$ and $\Theta_{\rm P}$ for three compounds. The antiferromagnetic nearest-neighbour exchange parameters and $\Theta_{\rm P}$ calculated using these parameters are also tabulated. (The other parameters are $D_{\rm Fe}/J_{\rm FeFe} = D_{\rm Mn}/J_{\rm MnMn} = 0.2$, $G_{\rm Fe}/J_{\rm FeFe} = G_{\rm Mn}/J_{\rm MnMn} = 0.18$, and $j = 0.2J_{\rm FeFe}$).

Sample	$T_{\rm cusp}$(experiment) (K)	$\Theta_{\rm P}$(experiment) (K)	$T_{\rm cusp}/S^2$	J (K)	$\Theta_{\rm P}$ (K)
$LuFeMgO_4$ [14]	33	$\simeq -600$	$0.23J_{\rm FeFe}$	23	-403[a]
$LuGaMnO_4$	11	$\simeq -150$	$0.23J_{\rm MnMn}$	7.7	-134[a]
$YFeMnO_4$ [15]	48 (60)[b]	$\simeq -800$	$0.29J_{\rm FeFe}$[c]	$J_{\rm FeFe} = 23$ $J_{\rm MnMn} = 7.7$ $J_{\rm FeMn} = 13.3$	-501[d]

[a] $\Theta_{\rm P} = -\frac{2}{3}(6cJ + 3cj)S(S+1)$, $c = 0.5$.
[b] Sample dependent; see the text.
[c] For the z-component.
[d] $\Theta_{\rm P} = -\frac{2}{3}(\frac{1}{2}(3J_{\rm FeFe} + 3J_{\rm MnMn} + 6J_{\rm FeMn}) + 3j)S(S+1)$.

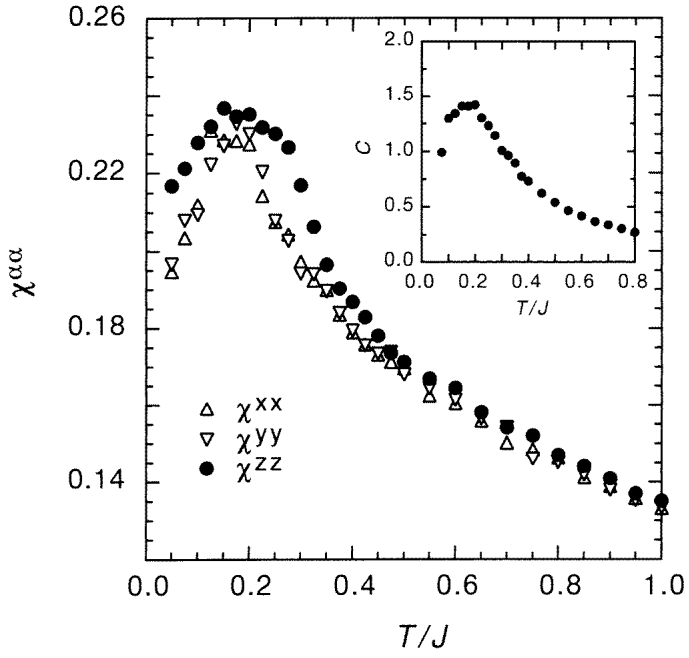

Figure 5. The uniform susceptibility for the model of $YFeMnO_4$ calculated using the parameters given in table 1. The arrows indicate $T_{\rm cusp}$ for the z- and xy-components. The inset shows the specific heat. The temperatures are scaled with respect to $J = J_{\rm FeFe}$ throughout this study.

observation. The parameters are summarized in table 1. In the simulation of the mixed system, all of the parameters and energies (temperatures) are scaled with respect to $J_{\rm FeFe}$. Therefore the simulated results will be shown with the temperatures scaled with respect to $J_{\rm FeFe}$ throughout this study. Note that the difference between the values of $T_{\rm cusp}$ for the two diluted compounds leads to $J_{\rm FeFe}$ having three times the magnitude of $J_{\rm MnMn}$. According to the empirical relation given in [19], a geometrical mean has been used for the interaction between Fe^{3+} and Mn^{2+}. The same ratio was used for both D and G; $D_{\rm Fe}/J_{\rm FeFe} = D_{\rm Mn}/J_{\rm MnMn} = 0.2$ and $G_{\rm Fe}/J_{\rm FeFe} = G_{\rm Mn}/J_{\rm MnMn} = 0.18$. For further

simplicity, the weak interlayer interaction j is assumed to be independent of the type of magnetic ion. The simulation was carried out for spins with unit length, but $S = \frac{5}{2}$ was used for the estimation of the parameters. The paramagnetic Curie temperatures Θ_P calculated using the estimated parameters and the experimental values are also compared in the table. The calculation gives a reasonable account of the observed high Θ_P as well as the low T_{cusp}.

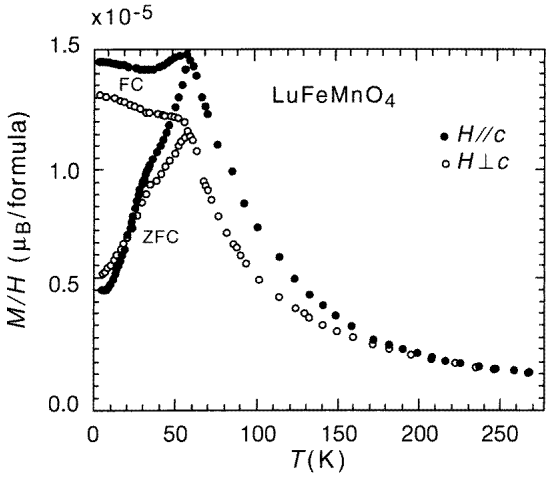

Figure 6. The dc susceptibility of a single crystal of $LuFeMnO_4$, whose magnetic properties are almost identical with those of $YFeMnO_4$.

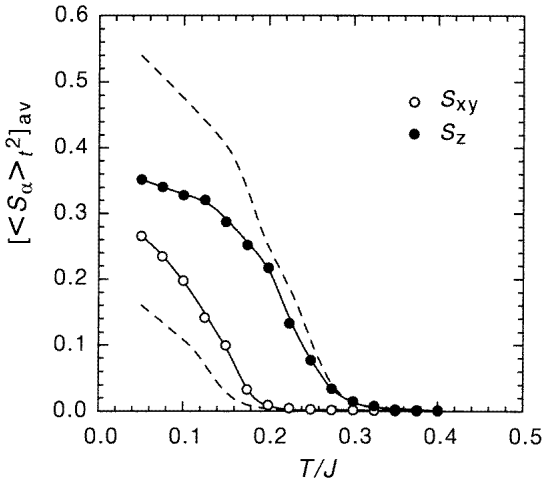

Figure 7. Time- and configuration-averaged spin components for the model of $YFeMnO_4$. The average of S_x and S_y is plotted for the in-plane component. The dotted lines represent the calculation without in-plane anisotropy.

The procedure of the simulation of the random mixed system is identical to that described in I. Employing a standard Metropolis method, several physical quantities were calculated for about 10 000 Monte Carlo steps (MCSs) subsequent to about 10 000 equilibrating steps. The calculations were carried out for $30 \times 30 \times 2$–$45 \times 45 \times 2$ lattices with periodic boundary

conditions. Averaging over 5–10 independent random ionic distributions was also carried out. The uniform susceptibilities calculated from the fluctuation of the magnetization are shown in figure 5 together with the specific heat calculated from the energy fluctuation. The experimental susceptibility for $LuFeMnO_4$ is also shown, in figure 6, for comparison. To illustrate the freezing behaviour, time- and configuration-averaged spin components are shown in figure 7, where the average is

$$[\langle S_\alpha \rangle_t^2]_{av} = \left\langle \left(\frac{1}{t_1 - t_0} \int_{t_0}^{t_1} S_\alpha(t)\ \mathrm{d}t \right)^2 \right\rangle_{\text{config}}. \tag{3}$$

Note that the in-plane anisotropy now leads to a consistent account of the nearly isotropic spin direction observed at the lowest temperature.

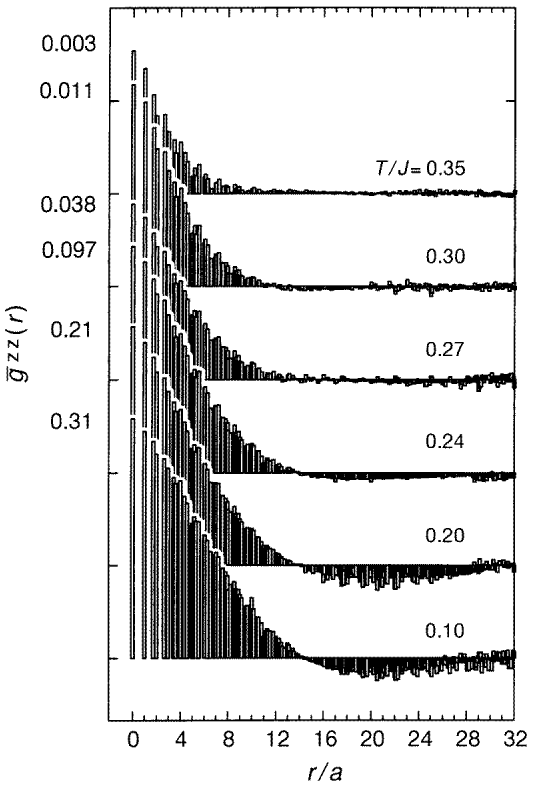

Figure 8. The temperature dependence of the amplitude (divided by the phase factor of the 120° structure) of the angle-averaged spin-correlation function for S_z. T_{cusp} for S_z is $0.29J$. The values on the left-hand side indicate $g^{zz}(0)$ at each temperature. The correlation functions were obtained from the time-averaged spin configurations averaged over 10 000 MCSs.

The experimentally observed T_{cusp} for $YFeMnO_4$ is somewhat dependent on the sample; a crystal of $YFeMnO_4$ grown recently gives a smaller value, 48 K [20, 21], than that obtained previously, 60 K [15]. The ICP analysis of the atomic composition (NTT Advanced Technology Incorporated) of the $YFeMnO_4$ crystals has shown that the sample with the lower T_{cusp} is more stoichiometric, with a molar ratio of 1.04:1:1.01:4.07. The observed value, $T_{\text{cusp}} = 48$ K, is in reasonable agreement with the value 42 K for freezing of the z-component obtained by this simulation.

4. Discussion and conclusions

It has already been found for $YFeMnO_4$ that a marked short-range spin correlation characterized by the wave vector $\boldsymbol{Q} = (\frac{1}{3}, \frac{1}{3}, \ell)$ exists at temperatures far higher than $T_{\rm cusp}$ in the magnetic neutron scattering, and that the short-range spin correlation does not show any anomaly at $T_{\rm cusp}$ [17]. The general features are the same as those found for the diluted system. It is thought, however, that the details of the spin correlation can be obtained by means of simulation, because the number density of magnetic ions is higher in this mixed system. The temperature variation of the spin-correlation function $g(r)$ calculated for the model of $YFeMnO_4$ is summarized in figure 8. The vertical bars indicate the amplitude of the angle-averaged correlation function $\bar{g}(r)$ apart from the phase factor of the uniform 120° structure. The $g(r)$s were obtained from the inverse transformation of the power spectrum of the time-averaged (not the instantaneous) spin configuration for a $64 \times 64 \times 2$ lattice. The time averaging was carried out for 10 000 MCSs and the averaging of the spectrum over typically ten independent random ionic distributions was also performed. A direct discrete Fourier transformation was individually performed for each triangular lattice. The simulation shows that the non-uniformity of the antiferromagnetic interaction estimated here actually prevents the transition to the long-range-ordered state (which occurs in the case of uniform interaction and anisotropy) from occurring, and leads to a well-defined short-range correlation. That the degree of short-range correlation itself gradually increases on cooling, and that there is no drastic change at $T_{\rm cusp}$ is totally consistent with the experimental results reported. The range of the correlation at $T/J = 0.30$, for example, is comparable to the experimental value ($\xi = \kappa^{-1} \simeq 21$ Å $\simeq 6a$ at $T = 81$ K) estimated from the reported magnetic scattering profile [17].

It was speculated in I that, at temperatures sufficiently below $T_{\rm cusp}$, there is a correlated

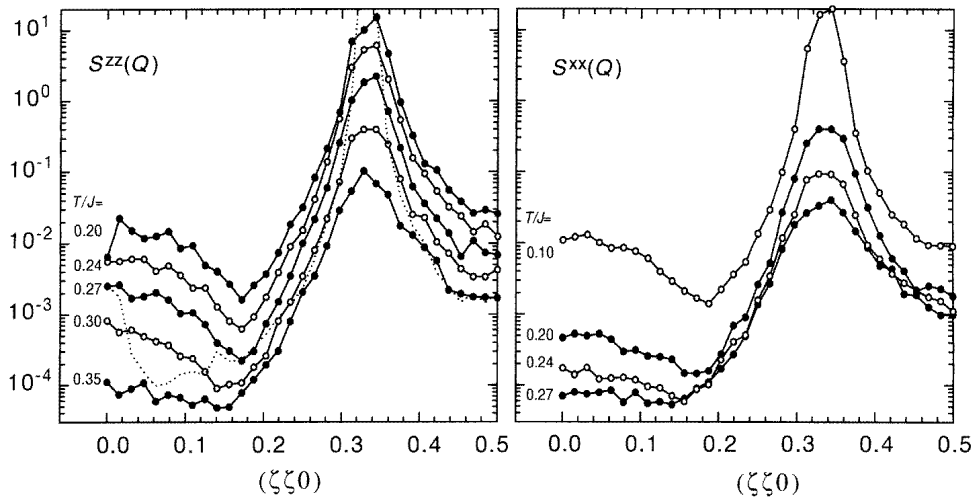

Figure 9. The temperature dependence of the power spectrum (scattering function) plotted along the [110] direction. These spectra were obtained from the same time-averaged spin configurations as were used for figure 8. The dotted line is the spectrum obtained for the (quasi-) long-range 120° structure in a 64×64 lattice with uniform exchange and anisotropy parameters. These figures demonstrate the enhancement of the intensity in the smaller-Q region in this random mixed system.

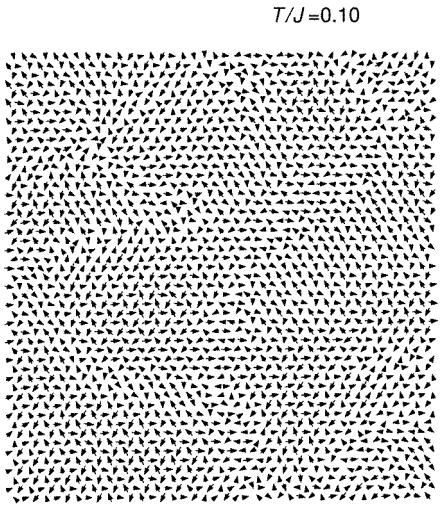

(a)

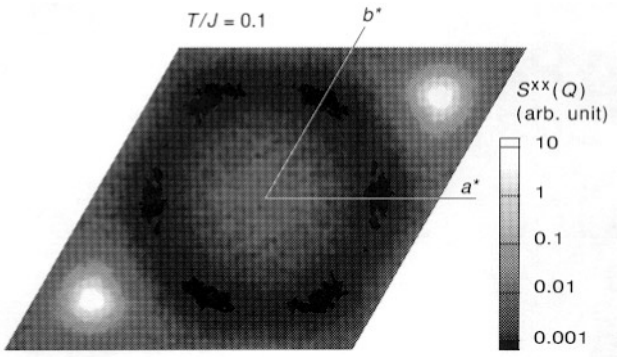

(b)

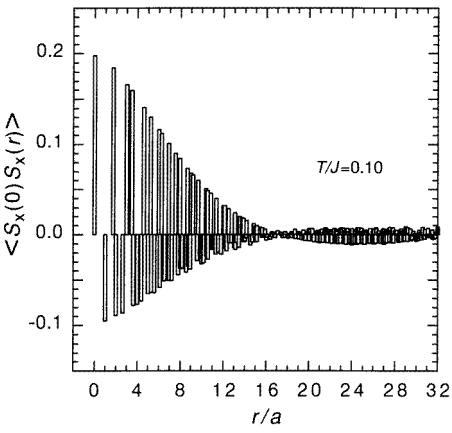

(c)

Figure 10. (a) Part of the low-temperature spin configuration in the xy-plane obtained at $T/J = 0.10$. (b) The corresponding power spectrum of S_x. (c) The correlation function obtained by inverse transformation of the power spectrum.

arrangement of domains with the short-range 120° structure. In the present mixed system, showing oscillatory behaviour of the amplitude, $\bar{g}(r)$ exhibits this structure more clearly. It has also been checked that this oscillatory behaviour is not an effect of the misfit at the boundary of the $64 \times 64 \times 2$ lattice. The temperature variations of the power spectra plotted along the [110] direction are summarized in figure 9. The correlation functions described above were calculated from these power spectra. Although the lattice size is not large enough for discussing the detailed structure in the reciprocal space, an enhancement of the scattering in the lower-Q region, rather than the $(\frac{1}{3}, \frac{1}{3}, 0)$ peak, is demonstrated. To illustrate the situation in real space, an example of the low-temperature ($T/J = 0.10$) spin configuration in the xy-plane obtained by gradual cooling from the initial random spin orientation is depicted in figure 10, together with the corresponding Fourier-transformed power spectrum for S_x and the inversely transformed correlation function $g^{xx}(r)$. In an experimental sense, figure 10(a) would represent the typical spin structure at the lowest temperature in this mixed system. As has been discussed in I, this higher-order structure is a manifestation of the residual degree of freedom in the orientation or phase of the short-range structure in the ground state, because the simultaneous ordering on cooling into a state with long-range phase coherence is not energetically allowed due to the 'homogeneous' randomness and the frustration.

In the vicinity of T_{cusp}, as seen in figure 8, the correlation function $\bar{g}(r)$ shows no structure, but a well-defined short-range order. Since, however, the Curie–Weiss-like susceptibility actually forms a cusp in the experiment and also in the simulation, a certain change in the spin correlation is expected. In I, the emergence of a long-range network of quasi-static spins out of the frustrating environment at T_{cusp} has been suggested. The same feature can also be seen in this mixed system. The quasi-static network which corresponds to the non-uniform spatial distribution of the relaxation time just below the freezing point is shown in figure 11. The bars in the figure indicate the lengths of time-averaged spins at $T/J = 0.27$, near the freezing point of the z-component in the model of $YFeMnO_4$. The three consecutive pictures correspond to the patterns averaged over the time windows of 16 000–24 000, 24 000–32 000, and 32 000–40 000 MCSs, respectively. Since the distribution is more uniform at higher temperatures, the formation of this non-uniform structure clearly corresponds to a well-known feature of the conventional spin glasses, i.e. the rapid broadening of the distribution of relaxation times upon freezing [22–24], and also to the formation of the cusp in the susceptibility. The wide distribution of relaxation times observed for this mixed system is again interpreted as a natural consequence of the randomness and the frustration of the short-range interactions, which prevent the simultaneous freezing of all spins.

It is difficult to prove whether or not these simulated distributions were obtained in the true equilibrium state, but it is possible to show that these patterns are statistically identical. Therefore the pictures suggest a temporal change of the spatial distribution of the relaxation time, or the dynamics of the network, on a timescale of ∼8000 MCSs, probably driven by thermal activation of the correlated region. It would be of some interest to interpret the experimentally observed properties on the hypothesis that this kind of excitation of 'non-uniformity' in the spatial distribution does not destroy the long-range network even in the two-dimensional lattices, but exists as a collective mode in the low-temperature phase. At least for qualitative interpretation of the experimental data, this intuitive description seems to contain no inconsistency. It should be noted that, if the slow change of the spatial distribution as observed in the simulation is accepted as an equilibrium property, the time-averaged quantity defined by equation (3), and also the autocorrelation of spins $\langle S_i(t)S_i(0)\rangle$, may vanish in the limit $t \to \infty$ even below T_{cusp}. This might suggest the

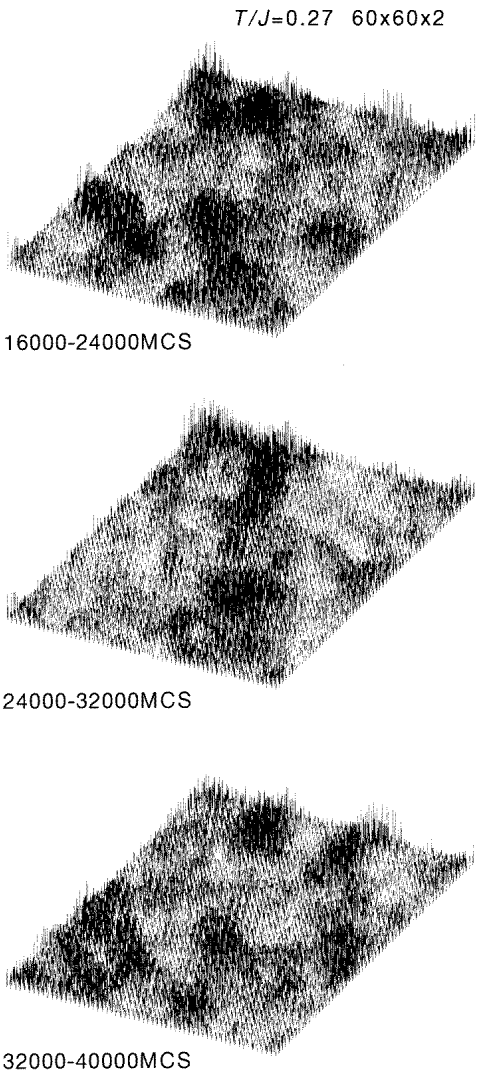

Figure 11. The temporal change of the time-averaged spin configuration just below T_{cusp}. The bars indicate the lengths of the spins after the time averaging over 8000 MCSs. The figure also shows the change of the spatial distribution of the relaxation times of the spins measured within the time window of 8000 MCSs.

possibility that a new order parameter which describes the spontaneous formation of the long-range connection at T_{cusp} can also describe the observed finite-temperature freezing in this quasi-two-dimensional system.

At temperatures sufficiently far below T_{cusp}, the excitation of the movement of the correlated domains or the antiphase boundary discussed before may also be possible. Because of the resemblance of this situation to the ordinary glassy state, however, the movement seems to be extremely slow in the state in which the domain correlation or the higher-order structure is well developed.

Although this intuitive discussion seems to be valuable in leading to an understanding of

the observed properties, more rigorous treatment will be necessary in order to establish the universality of the cooperative freezing in this random frustrated system. It is crucially important to elucidate the form of the collective dynamics in these random frustrated systems. We note that a mesoscopic domain theory of spin glasses [25] would also be instructive.

In conclusion, the experimentally observed spin-glass-like freezing in the triangular-lattice random mixed antiferromagnet $YFeMnO_4$ has been analysed by means of Monte Carlo simulation. New experimental results for diluted $LuGaMnO_4$ have also been presented. The exchange parameters in the model Hamiltonian have been estimated for random mixed $YFeMnO_4$ and random diluted $LuFeMgO_4$ and $LuGaMnO_4$. The model provides a qualitative interpretation of the observed spin freezing in the random mixed system $YFeMnO_4$, except the simultaneous freezing of the z- and xy-components of the spins.

The simulation actually shows that the non-uniform antiferromagnetic interaction due to the random distribution of Mn^{2+} and Fe^{3+} in $YFeMnO_4$ prevents there from being uniform long-range phase coherence of the triangular 120° structure. Instead, it causes well-defined short-range correlation and also a distribution of the relaxation times. It has also been shown that the susceptibility forms a cusp whereas the short-range spin correlation characterized by the wave vector $\boldsymbol{Q} = (\frac{1}{3}, \frac{1}{3}, \ell)$ does not show any abrupt change at T_{cusp}. Formation of the higher-order structure of the short-range correlation at temperatures lower than T_{cusp}, similarly to the case for the diluted system, has been clearly demonstrated. As regards the observed finite-temperature spin freezing in this system, the emergence of a long-range network of quasi-static spins at T_{cusp} is discussed.

Further study of these random frustrated systems under a external magnetic field will be valuable, because a novel response of the spin dynamics to external fields has been found in μSR and Mössbauer experiments [20, 26].

Acknowledgments

The authors thank Professor K Kohn, Professor J Akimitsu and Dr J Iida for sample preparation and magnetization measurements.

References

[1] Ikeda N, Kohn K, Himoto E and Tanaka M 1995 *J. Phys. Soc. Japan* **64** 4371
[2] Hirota K, Nakazawa Y and Ishikawa M 1991 *J. Phys.: Condens. Matter* **3** 4721
[3] Ramirez A P, Espinosa G P and Cooper A S 1990 *Phys. Rev. Lett.* **64** 2070
[4] Kurtz W 1982 *Solid State Commun.* **42** 871
[5] Dachs H and Kurtz W 1977 *J. Magn. Magn. Mater.* **4** 262
[6] de Seze L 1977 *J. Phys. C: Solid State Phys.* **10** L353
[7] Villain J 1979 *Z. Phys.* B **33** 31
[8] Todate Y, Himoto E, Kikuta C, Tanaka M and Suzuki J 1998 *Phys. Rev.* B **57** 485
[9] Morgenstern I and Binder K 1979 *Phys. Rev. Lett.* **43** 1615
[10] McMillan W L 1983 *Phys. Rev.* B **28** 5216
[11] Bray A J and Moore M A 1984 *J. Phys. C: Solid State Phys.* **17** L463
[12] Kimizuka N and Katsura T 1975 *J. Solid State Chem.* **13** 176
[13] Matsumoto T, Mori N, Iida J, Tanaka M, Shiratori K, Izumi F and Asano H 1992 *Physica* B **180+181** 603
[14] Tanaka M, Himoto E and Todate Y 1995 *J. Phys. Soc. Japan* **64** 2621
[15] Iida J, Tanaka M and Nakagawa Y 1990 *J. Phys. Soc. Japan* **59** 4443
[16] Wiedenmann A, Gunsser W, Rossat-Mignod J and Evrard M O 1983 *J. Magn. Magn. Mater.* **31–34** 1442
[17] Iida J, Tanaka M, Funahashi S and Nakagawa Y 1991 *J. Appl. Phys.* **69** 5801

[18] Casimir H B G, Smit J, Enz U, Fast J F, Wijn H P J, Gorter E W, Duyvesteyn A J W, Fast J D and de Jong J J 1959 *J. Physique Radium* **20** 360
[19] Cowley R A and Buyers W J L 1972 *Rev. Mod. Phys.* **44** 406
[20] Tanaka M, Todate Y, Natsume C, Nishiyama K and Nagamine K 1996 *Hyperfine Interact.* **97+98** 623
[21] Natsume C 1995 *Master Thesis* Ochanomizu University
[22] Murani A P 1981 *J. Magn. Magn. Mater.* **22** 271
[23] Uemura Y J, Yamazaki T, Harshman D R, Senba M and Ansaldo E J 1985 *Phys. Rev.* B **31** 546
[24] Dekker C, Arts A F M, de Wijn H W, van Duyneveldt A J and Mydosh J A 1989 *Phys. Rev.* B **40** 11 243
[25] Koper G J M and Hilhorst H J 1988 *J. Physique* **49** 429
[26] Todate Y, Ohnishi N, Tanaka M, Nishiyama K and Nagamine K 1997 *Hyperfine Interact.* **104** 375